

## **DESIGN FIGURES OF HIGH-TEMPERATURE LOW-PRESSURE COMBINED STEAM-CYCLE POWER UNIT**

**A.R. KVRIVISHVILI**

*Novosibirsk State Technical University, Novosibirsk, Russia*

*(Received July 10, 2006)*

The scheme and cycle of a promising highly economic coal-dust combined steam-cycle power unit are presented. The flow-rate, thermodynamic, and design figures of high-temperature sets (a coal-dust boiler and a high-temperature steam turbine) are considered.

### **1. BACKGROUND OF DEVELOPING AND INVESTIGATING COMBINED STEAM-CYCLE HIGH-TEMPERATURE LOW-PRESSURE POWER UNITS**

In the visible outlook, the coal will retain the positions of the main source for electric power production [1, 2]. In a number of developed countries, new highly efficient technologies of coal utilization based on integrated gasification combined cycle units (IGCC), combined cycle units (CCU) with pressurized fluidized bed combustion with external (indirect) combustion are developed within the framework of the national programs (ATS, Advanced Turbine Systems — USA, “THERMIE” — European Union, etc.). The efficiency of such units reaches 45–50 %.

In the IGCC scheme the synthesis-gas obtained in the gasifier is burnt in the gas-turbine stage after the gas cleaning, and the gases with temperatures of 450–500 °C emanating from the gas turbine are directed to the Heat-Recovery Steam Generator (HRSG) of the steam-turbine stage.

In the coal CCU with pressurized fluidized bed combustion scheme steam is generated in the power boiler for the steam turbine stage, and the escaping gases are expanded in the gas turbine after their gas cleaning.

In the scheme of coal CCU with the external (indirect) combustion, the power air boiler, in which a hot air (as the working body) under pressure supplied to the gas turbine and then to the HRSG of the steam-turbine stage is generated, is the combustion chamber of the gas-turbine stage (GTU — gas-turbine unit). The hot air expands in the gas turbine. The coal combustion and the cleaning of combustion gases are carried out under the atmospheric pressure (as in conventional boilers). The GTU power units with an external combustion and power of 12.5 MW operate at coal-dust power plants in Saint-Denis (France), Dundee (Scotland), Oberhausen (Germany), and with power of 10 MW at the Kashira Thermoelectric Plant (on the brown coal). The air is heated up to 1090–1260 °C in the ceramic heat exchangers of the air boiler. An increase in the air temperature in the boiler up to 1650 °C is believed to be promising [3]. It is envisaged to

mount a demonstration power unit with an external staged coal combustion 20 MW at the Burren thermoelectric plant in Pennsylvania which operates on hot air.

A CCU with power of 280–320 MW and indirect coal combustion and air heating up to 1090 °C in a boiler with ceramic heat exchangers was developed within the program “Pure coal” (USA) [3]. The achieved efficiency reached 49–51 %.

The advanced design materials such as the chromium-nickel and chromium-aluminum steels, dispersion composites based on nickel, its alloys, and chromium, the eutectic niobium-based composites, the composite ceramics [4, 5, 6] may be used in the CCU for power carriers at temperatures of 1200–1600 °C.

The U.S. Department of Energy has developed the power program “Vision 21” [7] for the use of ceramics in high-temperature power engineering processes. The Rolls-Royce (USA), Solar Turbines, Inc. (USA) firms study the turbine ceramic blades on the 501K and Centaur 50S engines, respectively.

The working temperatures of ceramic materials of complex composition approach 1700–1800 °C, and the strength is maintained nearly invariable at the level of 45–55 MPa. The pipes of  $\text{Si}_3\text{N}_4$ –MgO composite ceramics have an allowable wall temperature of 1400 °C, and for  $\text{SiC}$ – $\text{Al}_2\text{O}_3$  this temperature is 1600 °C. The heatproof heat-resistant design aluminum-boron-nitride ceramics with the working temperature up to 1600 °C has been developed at the scientific-engineering center “Ceramic thermal engines” of the Scientific-Research Technical Institute of Power Engineering (St. Petersburg) and a highly efficient metal-ceramic stationary gas-turbine engine with power of 2.5 MW is under development [6]. Such elements as the casings, the combustion chamber, gas pipes have already been manufactured and tested. The centrifugal compressor, the shaft, the directing apparatus, the disk and the bladed work wheel made up of metal ceramics are prepared for tests.

The price of ceramic materials amounts from 10 to 50 % of the cost of high-temperature metals according to the estimates of [5]. The production of a wide range of smooth and ribbed ceramic pipes and panels has already been mastered abroad. These products are used in the regenerators and air boilers operating in the GTU and CCU schemes.

The use of high-temperature low-pressure combined steam-cycle power units (CSCPU, Fig. 1), operating in a combined cycle proposed in the work [8], which combines the Field — Baranovsky cycle [9] in the high-temperature low-pressure steam turbine

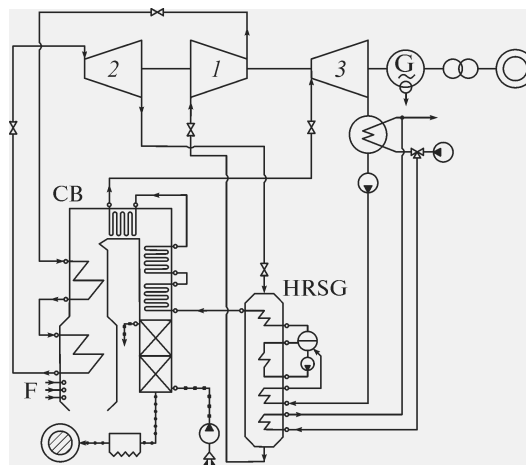


Fig. 1. Schematic of a combined steam-cycle power unit.

1 — steam compressor, 2 — high-temperature steam turbine, 3 — heat-recovery steam turbine, CB — coal-dust boiler, HRSG — heat-recovery steam generator, G — generator, F — fuel supply.

Fig. 2. The combined steam-cycle power unit cycle in the  $T, S$  diagram:  $A, B, C, D, E, O, K, K'$  are the cycle characteristic points.

stage and the Rankine cycle in the heat-recovery part (Fig. 2), is a further development of the coal CCUs with external combustion.

The composition of facilities, which might realize the proposed combination of cycles, was not developed until now neither in the native nor in world practice. Along with this, the efficiency of such a power unit has been shown by computations to amount to 50 %, therefore, the development and investigation of the CSCPU are topical.

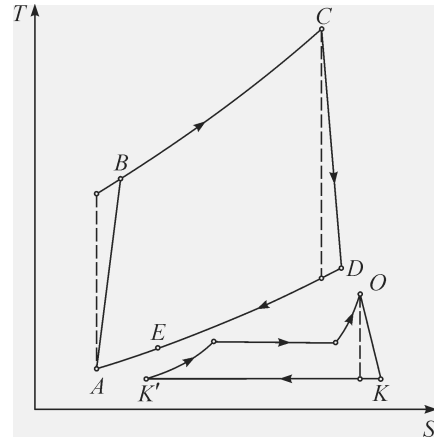
According to the CSCPU scheme (see Fig. 1) the steam under a pressure, for example, of 0.05–1 bar is compressed in the compressor (in the process  $A, B$ ) up to a pressure of 5–15 bar, is overheated in the process  $B, C$  up to 1100–1400 °C in the generating surfaces of the coal-dust boiler and is fed into a high-temperature low-pressure steam turbine, in which it expands (in the process  $C, D$ ). With a temperature of 550–700 °C (at the end of the expansion process) the steam is supplied to the HRSG, where it cools down in the process  $D, E$  and generates a steam with temperature of 250–300 °C with its further increase up to 500–550 °C in the steam overheater of the coal-dust boiler. The state ( $A$ ) ahead of the compressor is (generally) reached by cooling the steam (in the process  $E, A$ ) with the heat removal by cooling water. The high-temperature contour is closed. The relative steam flow rate in the heat-recovery contour equals  $\beta = 0.3\text{--}0.4$ . The CSCPU efficiency in terms of electric power output is

$$\eta_N = \frac{l_T - l_{Cm} + l_\beta}{h_C - h_B + \beta(h_0 - h_{UB})} \eta_K \eta_{TP} \eta_{EM} \eta_{aux},$$

where  $l_T = h_C - h_D$  is the high-temperature turbine work, kJ/kg,  $l_{Cm} = h_B - h_A$  is the steam compressor work, kJ/kg,  $l_\beta = \beta(h_0 - h_K)$  is the heat-recovery turbine work, kJ/kg,  $h_A, h_B, h_C, h_D, h_0, h_K$  are the enthalpies at characteristic points (see Fig. 2) of the cycle, kJ/kg,  $h_{UB}$  is the enthalpy of the heat-recovery contour steam at the HRSG outlet, kJ/kg,  $\eta_K, \eta_{TP}, \eta_{PT}$ , and  $\eta_{aux}$  are the efficiencies of the coal-dust boiler, power transport, electric mechanic efficiency, and of auxiliary needs.

## 2. HIGH-TEMPERATURE CSCPU SETS

Basic peculiarities of the development of high-temperature low-pressure sets (the boiler, the turbine) are determined by steam parameters. At the initial parameters of 5–11 bar, 1000–1200 °C the steam has a specific volume of 0.5–1.4 m<sup>3</sup>/kg, which causes the inclusion in collectors of a large number of concurrently operating shield pipes at the steam velocities of 22–27 m/s, the five-percent (of the steam initial pressure) hydraulic resistance and the use of doubled staggered plain-pipe wall heating surface, which are additionally due to the heat transfer coefficients from the wall to the superheated steam at the level of 200–250 W/(m<sup>2</sup>·K), low temperature levels at the cold and hot ends of the heating surfaces and, as a consequence, leading to thermal stresses of shield surfaces 15–20 kW/m<sup>2</sup> and to a high furnace of the boiler (for the



U-shaped arrangement). The packages of pipes of convective heating surfaces are connected with one another by ducts (similarly to air ducts in the air heater).

All the stages of the high-temperature low-pressure steam turbine are subsonic (there are no wave losses) at the sound velocity of 715–910 m/s and heat drop of 150–230 kJ/kg, which causes (with regard for optimal partitioning of the heat drop in stages and technological constraints) a root diameter of 1.4–1.6 m and the rotor dimensions commensurable with the dimensions of rotors of the conventional low-pressure cylinders. The Reynolds numbers (Re) for the steam flow through the nozzle and working cascades of blades go beyond the self-similar regime, therefore, the corrections for Re were taken into account when determining the generalized aerodynamic characteristics.

The developed mathematical models of the functioning of high-temperature low-pressure sets (of the boiler and turbine) are based on the equations:

– of energy balance

$$BQ_i^r = \sum_{k \in V(i)} (\eta G^x h)_{ki} - \sum_{j \in W(i)} (\eta G^y h)_{ij} = 0,$$

– of flow-rate balance

$$B + \sum_{k \in V(i)} G_{ki}^x - \sum_{j \in W(i)} G_{ij}^y = 0,$$

where  $B$  is the fuel flow rate,  $G$  and  $h$  are the flow rate and the enthalpy of the power carrier,  $\eta$  is the coefficient accounting for corresponding power losses,  $V(i)$  and  $W(i)$  are the sets of inlets and outlets of the set.

For each power carrier (depending on the design and arrangement figures  $X^K$  and flow-rate and thermodynamic parameters  $X^P$ ), the equations are written:

– of the enthalpy change

$$\Delta h_j = \Delta h_j(X^K, X^P),$$

– of the pressure change

$$\Delta p_j = \Delta p_j(X^K, X^P),$$

– of the temperature change

$$\Delta t_j = \Delta t_j(X^K, X^P),$$

– of the coefficient accounting for energy losses,

$$\eta_j = \eta_j(X^K, X^P),$$

– of the mean flow velocity

$$\omega_j = \omega_j(X^K, X^P).$$

For each  $q$ th element manufactured from the  $m$ th construction material, the dependencies are formulated:

– of the highest surface temperature

$$t_{qm} = t_{qm}(X^K, X^P),$$

– of the wall thickness

$$\delta_{qm} = \delta_{qm}(X^K, X^P),$$

– of arising integral stresses and bending stresses

$$\sigma_{qm}^{\Sigma} = \sigma_{qm}^{\Sigma}(X^K, X^P),$$

$$\sigma_{qm}^b = \sigma_{qm}^b(X^K, X^P),$$

– of metal expense

$$G_{qm} = G_{qm}(X^K, X^P).$$

The constraints taking into account the technological convenience, operation reliability, and conditions for physical-technical processes are imposed on the figures and parameters:

$$X^{K*} \leq X^K \leq X^{K**},$$

$$X^{P*} \leq X^P \leq X^{P**},$$

$$\omega_j^* \leq \omega_j(X^K, X^P) \leq \omega_j^{**},$$

$$\Delta t_j^* \leq \Delta t_j(X^K, X^P) \leq \Delta t_j^{**},$$

$$\eta_j^* \leq \eta_j(X^K, X^P) \leq \eta_j^{**},$$

$$t_{qm}^* \leq t_{qm}(X^K, X^P) \leq t_{qm}^{**},$$

$$\delta_{qm}^* \leq \delta_{qm}(X^K, X^P) \leq \delta_{qm}^{**},$$

$$\sigma_{qm}^{\Sigma*} \leq \sigma_{qm}^{\Sigma}(X^K, X^P) \leq \sigma_{qm}^{\Sigma**},$$

$$\sigma_{qm}^{b*} \leq \sigma_{qm}^b(X^K, X^P) \leq \sigma_{qm}^{b**},$$

$$F^n = \{X^K, X^P \mid f_n(X^K, X^P) \geq 0\},$$

where  $n$  is the dimension of the vector of the values of variables  $X^P$ .

The heat exchange peculiarities in the boiler furnace are taken into account by using the equation [10, 11]

$$\varphi(V_c)(T_a - T_T'') = \frac{1}{B} c_0 a_T F_3 \left\{ \left[ T_F'' (1 + \sum \Delta_i) \right]^4 - \left[ T_{p.c} + \left( \varepsilon + \frac{1}{\alpha_2} \right) \frac{B \varphi(V_c)(T_a - T_T'')}{10^{-3} F_3} \right] \right\},$$

where  $V_c$  is the mean heat capacity of gases,  $T_a$ ,  $T_T''$ , and  $T_{p.c}$  are the adiabatic (combustion) temperature, the temperature at the furnace end, and the (mean) temperature of steam in pipes,  $c_0$  is the coefficient of the absolutely black body radiation,  $a_F$  is the reduced blackness degree of the furnace,  $F_3$  is the area of shield pipes,  $\sum \Delta_i$  are the computational corrections,  $\varepsilon$  is the thermal resistance of the pollution,  $\alpha_2$  is the coefficient of heat transfer from the wall to the superheated steam,  $\varphi$  is the heat conservation coefficient.

The turbine profile peculiarities are taken into account using the dependencies [12, 13]

$$l_1^3 + 2d_r l_1^2 + d_r^2 l_1 - \frac{G_0 v_{lt}(u/c_f)}{\mu_1 e \pi^2 \sin \alpha_{1ef} n \sqrt{1 - \rho_{mean}}} = 0,$$

$$(d_r + l_2)l_2 = \frac{G_0 v_2}{\pi \sqrt{0.03 H_{00}}},$$

where  $H_{00}$  is the available heat drop on the turbine,  $v_2 \approx v_e$  is the steam specific volume at the outlet of the last stage,  $v_{1t}$  is the specific volume at the outlet of the nozzle grate,  $e$  is the partiality degree, at a throttle steam distribution it equals 1,  $\mu_1$  is the flow rate coefficient,  $G_0$  is the steam flow rate via the stage,  $u/c_f$  is the ratio of velocities for a stage,

$d_r$  is the root diameter,  $\alpha_{1ef}$  is the effective angle of the nozzle outlet,  $n$  is the frequency of turbine rotation,  $\rho_{mean}$  is the reaction degree over the mean diameter,  $l_1$ ,  $l_2$  are the heights of the nozzle blade of the first stage and the rotor blade of the last stage.

### 3. COMPUTATIONAL RESULTS

Using the developed mathematical model of the CSCPU functioning at thermoelectric plants a series of computations was performed for condensing power units with power of 25–65 MW at their operation on the Kuznetsk coal of the rank “G” and the steam parameters presented in Table 1. For the boiler and turbine elements, the following construction materials are adopted: the wall shield pipes 0.06 m in diameter — the composite ceramics  $\text{Si}_3\text{N}_4\text{--MgO}$ , the pipes 0.06 m in diameter of the convective steam overheater — Cr–Ni–Ti steel, the pipes 0.038 m in diameter of the convective steam overheater of the heat-recovery contour — Cr–Mo steel, the pipes of air heater 0.04 m in diameter — steel 20, the blades of the turbine stages — Cr–Ni high alloys steel rotor — the Ni–Mo–V alloy, the casing — Cr–Ni–Ti steel.

Strength computations were carried out by the technique from [14]. The turbine rotor mass was estimated from a regression dependence obtained on the basis of data of [15, 16]. The investments in the aggregates were calculated on the basis of methodic approaches of [17] and the costs of construction materials: the composite ceramics — 3 doll/kg, Cr–Ni–Ti steel — 5 doll/kg, Cr–Mo steel — 3 doll/kg, steel 20 — 2 doll/kg, Cr–Ni high alloys (on the average) — 110 doll/kg, Ni–Mo–V, Cr–Ni–Ti steel — 8 doll/kg.

As an example, Fig. 3 shows the design arrangement scheme, and Table 2 presents the mass and overall dimension parameters of high-temperature low-pressure boilers. It follows from these data that the height of the furnace and the packages of heating surfaces depends little on the steam productivity for a U-shaped arrangement of boilers, because the transverse overall dimensions grow with the increasing steam productivity. The CSCPU boilers have the furnace combustion intensity which is by a factor of about 1.6–2.6 lower than for the conventional steam boilers of the same steam productivity.

Along with this, such a lower combustion intensity of chambers is no restricting factor for a normal process of fuel combustion and the functioning of shields because the minimum temperature of the wall of shield pipes will be at the level of 800–850 °C at the effective temperature of 1200–1300 °C at the furnace medium.

Table 1

Basic parameters of the CSCPU

Parameters	Working body states						
	A	B	C	D	0	K	K'
Pressure, bars	0.3	8.4	8	0.33	35	0.05	0.05
Temperature, °C	79	534	1200	598	535	33	33
Entropy, kJ/(kg·K)	7.82	7.94	9.39	9.61	7.26	7.69	0.48
Enthalpy, kJ/kg	2644	3555	5149	3701	3531	2345	137.8

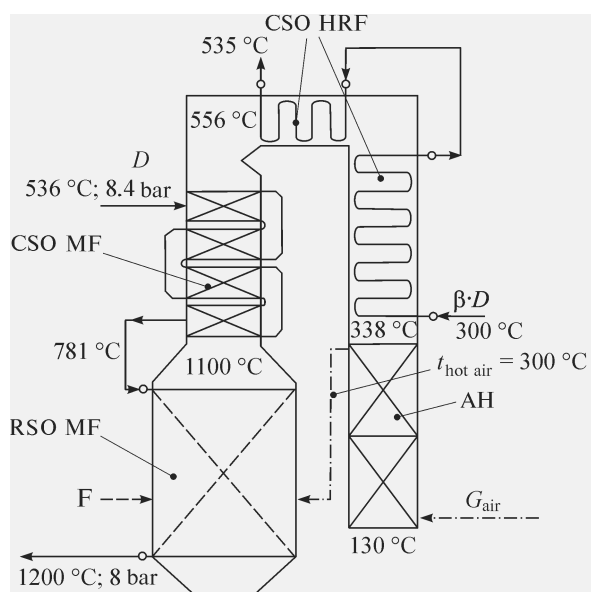


Fig. 3. Arrangement scheme of a high-temperature boiler.

RSO MF — the radiation steam overheater of the main flow, CSO MF — the convective steam overheater of the main flow, CSO HRF — the convective steam overheater of the heat-recovery steam flow, AH — the air heater,  $G_{\text{air}}$  — the air flow rate,  $F$  — fuel supply,  $D$  — the steam flow rate of the high-temperature contour,  $t_{\text{hot air}}$  — the air temperature at the AH outlet.

Table 2

Mass and overall dimension parameter of high-temperature low-pressure coal-dust boilers

Furnace	Power unit capacity, MW		
	27	45	63
Boiler steam productivity, t/h	104	168	242
Furnace width, m	5.67	10.08	13.77
Furnace depth, m	5.4	8.2	11.7
Furnace height, m	19.7	18.9	18.5
Number of packages of pipes in CSO MF*, pcs	23	23	22
Number of pipe rows in CSO MF* package, pcs	7	6	6
CSO MF* height, m	15.1	13.1	13.8
CSO HRF** height, m	15.6	15.6	15.4
Air heater height, m	13.7	13.6	13.8
Number of pipes operating in parallel			
RSO MF	480	790	1120
CSO MF	259	441	606
CSO HRF	72	106	168
AH	3276	5680	7616
Mass, t,			
RSO MF	36.5	52.6	92.6
CSO MF	66.6	109.2	160.4
RSO HRF	63.6	82.6	151.3
AH	59.8	92.7	140.0

\* MF — main flow, \*\* HRF — heat-recovery flow.

Table 3

## Gasdynamic and aerodynamic characteristics of HT-turbines with power of 40–95 MW

Parameters	Value
Available steam drop per one stage, kJ/kg	150–220
Absolute flow velocity at the nozzle outlet, m/s	450–560
Relative flow velocity at the rotor blade outlet, m/s	310–470
Absolute flow velocity at the rotor blade outlet, m/s	120–220
Mach numbers in nozzle arrays	0.6–0.7
Mach numbers in working arrays	0.4–0.7
Velocity coefficients of the nozzle array	0.96–0.97
Velocity coefficients of the working array	0.93–0.95
Flow-rate coefficients of the nozzle array	0.96–0.97
Flow-rate coefficients of the working array	0.94–0.95
Angle of flow entrance in the nozzle array, deg	13–20
Angle of flow entrance in the working array, deg	20–25
Number $10^{-5} \cdot Re_1$ for the nozzle array	2–10
Number $10^{-5} \cdot Re_2$ for the working array	1.4–6.8

Table 4

## Parameters of HT-turbines

Parameters	Power unit capacity, MW		
	27	45	63
Proper power of the HT-turbine, MW	40	66	95
Number of stages, pcs	11	9	9
Root diameter of blades, m	1.45	1.6	1.6
Internal relative efficiency of the turbine, %	88.29	88.69	89.62
Turbine rotor mass, t	34.1	35.8	35.8
Turbine casing mass, t	8.2	11.1	14.1
Blading mass, t	5.1	5.6	11.3

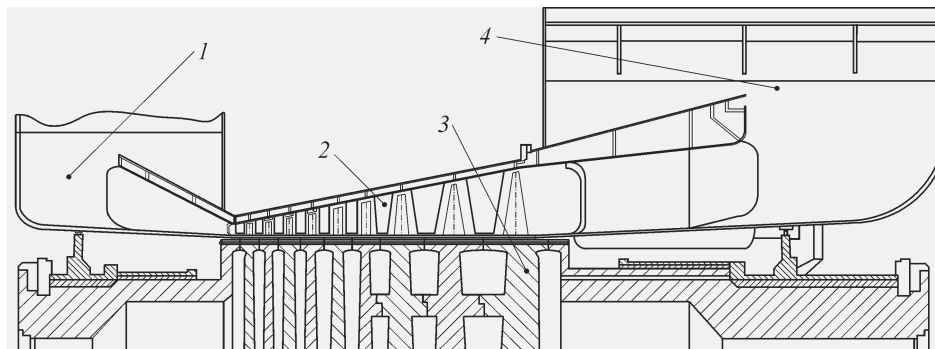


Fig. 4. Design and arrangement schematic of a high-temperature turbine with power of 66 MW.

1 — the inlet duct, 2 — the flow part, 3 — rotor, 4 — the outlet duct.



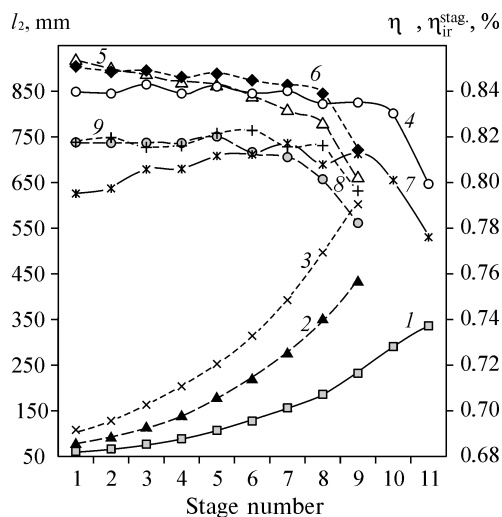


Fig. 5. The height of working blades  $l_2$  (lines 1–3), of the relative blade efficiency  $\eta_{rb}$  (lines 4–6) and the internal relative efficiency of the stage  $\eta_{ir}^{stag}$  (lines 7–9) vs. the stage number of HT-turbines: 40 (lines 1, 4, 7), 66 (lines 2, 5, 8) and 95 (lines 3, 6, 9) MW.

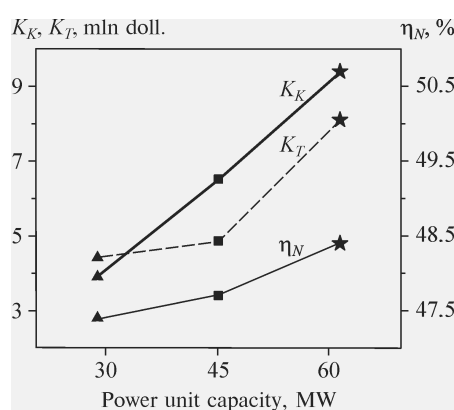


Fig. 6. Investments in high-temperature sets (boiler  $K_K$  and turbine  $K_T$ ) and the net efficiency ( $\eta_N$ ) of the CSCPU.

VVP: 27 (▲), 45 (■), 63 (★) MW.

in Fig. 4. It follows from these data that the available heat drop per stage is commensurable with the heat drop for stages of the low-pressure cylinders of conventional turbines. As a result, at nearly the same available heat drop per a turbine the number of stages of the HT turbine is by a factor of 2–2.5 less than the number of stages of a conventional steam turbine. Along with this, the internal relative efficiency of the HT turbine will be at the level of 0.88–0.90 despite a relatively low (0.80–0.82) efficiency of stages (Fig. 5), which is due to a high coefficient of the heat return (nearly 10 %). One can note that the efficiency of stages (and of the turbine on the whole) will be higher with increasing number of stages (decrease of the heat drop per stage) at nearly the same heights of blades and reaction degrees of stages 0.1–0.5.

Figure 6 shows the investments in high-temperature CSCPU sets and the net efficiency. It is seen from these data that the thermal efficiency of CSCPU may be at the level of 48 %, and the specific investments in high-temperature sets (the boiler and turbine) per one installed kW of CSCPU will amount to 280–310 doll/kW.

## CONCLUSIONS

1. A new highly efficient coal-dust technology has been proposed, which is based on the combination of Field — Baranovsky and Rankine cycles, and whose efficiency makes 48–50 %. A technique has been developed for computing the CSCPU, and a mathematical model has been created, which accounts for the peculiarities of computation of high-temperature sets.

2. The multi-variant computations have been performed, and the design and arrangement parameters together with the estimates of investments for coal-dust low-pressure boilers with high-temperature generating surfaces and HT-turbines operating within the power units with capacity of 25–65 MW have been obtained.

3. The coal-dust boiler is in terms of their external dimensions about 2 times larger than the conventional boilers of the same productivity, and the HT-turbines are commensurable with the low-pressure cylinders of conventional turbines. High temperatures and low pressures of the working medium enable the use of composite ceramics as the material for shield pipes, and one can use for the turbine blades the heatproof alloys based on nickel and nickel-cobalt.

4. Specific investments into the high-temperature sets (the boiler and the high-temperature steam turbine) per one installed kilowatt of the CSCPU amount to 280–310 doll/kW.

#### REFERENCES

1. **A.D. Goldstein, G.I. Pozgalev, and V.I. Dobrokhotoy.** State of the development of CCU on solid fuel, *Heat Power Engineering*, 2003, No. 2, P. 16–23.
2. **A.A. Salamov,** Development of thermoelectric plants operating on coal, *Ibid.*, 2000, No. 8, P. 75–76.
3. **G.G. Olkhovsky,** Development of promising GTUs in USA, *Ibid.*, 1994, No. 9, P. 61–69.
4. **Construction Materials: Handbook,** B.N. Arzamasov (Ed.), Mashinostroenie, Moscow, 1990.
5. **I.I. Kirillov, A.V. Sudarev, and A.G. Reznikov,** Ceramics in high-temperature GTUs, *Industrial Heat Technology*, 1988, Vol. 10, No. 6, P. 67–87.
6. **A. Sudarev, V. Tikhoplav, G. Shishov, and V. Katenev,** High-temperature engines using construction ceramics, *Gas-Turbine Technologies*, 2000, No. 3, P. 2–5.
7. **D. Derinsky,** Vision 21 — partnership of state and industry, *Ibid.*, 2000, No. 1, P. 16–22.
8. **A.R. Kvrivishvili,** Flow-rate, thermodynamic, and design and arrangement parameters of a coal-dust boiler of a combined steam-cycle power unit, in: *Power Systems, Power Plants, and Their Aggregates: Coll. Sci. Works*, V.E. Nakoryakov (Ed.), Novosibirsk State Tech. Univ., Novosibirsk, 2005, Iss. 9, P. 130–138.
9. **S.A. Aksyutin,** Prospects for Development of Steam and Gas Turbines of Electric Power Plants, Mashgiz, Moscow, 1957.
10. **Thermal Calculation of Boilers (Normative Method)**, 3rd Ed., NPO TsKTI, St. Petersburg, 1998.
11. **Yu.M. Lipov et al.,** Arrangement and Thermal Design of Steam Generator: A Textbook for Higher Schools, Energiya, Moscow, 1975.
12. **A.V. Shcheglyayev,** Steam Turbines. Theory of Thermal Process and Designs of Turbines, in 2 Books, Energoatomizdat, Moscow, 1993.
13. **L.V. Arsenyev, V.G. Tyryshkin, I.A. Bogov et al.,** Stationary Gas-Turbine Units, L.V. Arsenyev and V.G. Tyryshkin (Eds.), Mashinostroenie, Leningrad, 1989.
14. **G.S. Zhiritsky and V.A. Strunkin,** Design and Computation for Strength of Details of Steam and Gas Turbines, Mashinostroenie, Moscow, 1968.
15. **P.N. Shlyakhin and M.L. Bershadsky,** Brief Handbook on Steam Turbine Units, Energiya, Moscow, 1970.
16. **Yu.F. Kosyak, V.N. Galatsan, and V.A. Paley,** Operation of Turbines of Nuclear Power Plants, Energoatomizdat, Moscow, 1983.
17. **N.G. Zykova,** Scheme-parametric solutions for boilers of thermoelectric plants with annular fire-chamber, in: *Power Systems, Electric Power Plants, and Their Aggregates. Coll. of Sci. Works Novosibirsk State Tech. Univ.*, Novosibirsk, 2003, Iss. 8, P. 82–93.